International Journal of Mass Spectrometry 310 (2012) 10–19

Contents lists available at SciVerse ScienceDirect

International Journal of Mass Spectrometry

journal homepage: www.elsevier.com/locate/ijms

Development of PTR-MS selectivity for structural isomers: Monoterpenes as a case study

P.K. Misztal[a,b], M.R. Heal[b], E. Nemitz[a], J.N. Cape[a,*]

[a] Centre for Ecology & Hydrology, Penicuik EH26 0QB, UK
[b] School of Chemistry, University of Edinburgh, Edinburgh EH9 3JJ, UK

ARTICLE INFO

Article history:
Received 3 October 2011
Received in revised form 1 November 2011
Accepted 1 November 2011
Available online 7 November 2011

Keywords:
Fragmentation
Scanning voltage
Positive matrix factorization
Terpene

ABSTRACT

Proton-Transfer-Reaction Mass Spectrometry (PTR-MS) is a very useful tool for high frequency detection and quantification of gas-phase volatile organic compounds (VOCs) but the soft ionization means it is difficult to discriminate structural isomers. For example, to date it has only been possible to measure the sum of monoterpene concentrations, which have been monitored most commonly at *m*/*z* 81 and 137 at a constant drift voltage and pressure. We show here that PTR-MS is capable of discriminating individual monoterpenes when operating in the alternating drift voltage (AD) mode. The approach is based on the principle that slightly different energies are required for the fragmentation/clustering of a given monoterpene, so in AD mode each monoterpene has different time points for fragmentation. Therefore from a fragmentation analysis of background-subtracted standards it is possible to calculate the percentage of each monoterpene in an absolute concentration of their sum. Although monoterpenes have been chosen as an example, the method is likely to be effective for other structural isomeric species such as the sesquiterpenes or methyl vinyl ketone/methacrolein (MVK/MACR).

1. Fragmentation regimes in PTR-MS

Proton transfer reaction mass spectrometry uses a soft ionization technique in which hydronium ions (H_3O^+), formed in the hollow cathode of the ion source, ionize the target molecules of interest by proton transfer. Proton transfer only occurs to molecules for which the proton affinity is greater than that of water. The products of the proton transfer reactions are either protonated compounds or their protonated fragments or clusters. The magnitude of fragmentation/clustering can be optimised by adjusting the electric field (E) and the buffer gas number density (N) in the drift tube, so that the E/N ratio is most commonly in the range of 120–140 Td (1 Td = 10^{-17} V cm^2). For a fixed drift tube pressure and temperature the ratio E/N is directly proportional to the drift voltage (U_d).

Monoterpene concentrations, expressed as a total sum of isomers, have been shown to be measurable reliably by PTR-MS [1–4]. The sensitivity of the technique is dependent on the ambient humidity [5,6] and drift tube conditions, which regulate the proportion of signal at *m*/*z* 81 and *m*/*z* 137. This proportion can have diurnal variations but generally the sum of these ions should be more or less constant, provided no other compounds contribute significantly to the signal at these *m*/*z*. There have been attempts to unravel the information behind monoterpene fragmentation but there has been little progress in improving PTR-MS specificity in this respect. For example, Maleknia et al. [7] showed different abundances of monoterpenes and related compounds depending on the drift voltage used, and tested at *m*/*z* channels 155, 137, 135, 121, 119, 109, 107, 95, 93, and 81. Although practically all the monoterpenes tested (except for p-cymene), including related compounds such as oxygenated monoterpenes (linalool, 1,8-cineole), gave high abundance signals at *m*/*z* 81, not all the species had equally abundant signals at *m*/*z* 137. Interestingly, other *m*/*z* channels in addition to 81 and 137 showed a big variability in abundance with particular monoterpenes. The drift voltage (U_d) used was 580 V, at temperatures between 30 and 60 °C and drift tube pressures close to 200 Pa, equivalent to $E/N \sim 120$ Td, and the same authors repeated the study at 480 V and 380 V, but only for p-cymene and 1,8-cineole. The fragmentation of p-cymene is interesting because its protonated molecular ion detected at *m*/*z* 135 had the lowest abundance at high U_d (580 V), with only 4.3% abundance relative to the fragment ion at *m*/*z* 93. Decreasing U_d by 100 V caused a shift in the fragmentation such that the relative abundance increased to 55%. This was consistent with the study of Tani et al. [6] who measured 42% abundance at *m*/*z* 135 relative to *m*/*z* 93 at similar E/N conditions (120 Td). However, decreasing further the drift voltage by 100 V (i.e. to 380 V) resulted in the abundance of the parent ion at *m*/*z*

* Corresponding author. Tel.: +44 131 445 8533; fax: +44 131 445 3943.
E-mail address: jnc@ceh.ac.uk (J.N. Cape).

1387-3806/$ – see front matter © 2011 Elsevier B.V. All rights reserved.
doi:10.1016/j.ijms.2011.11.001

135 exceeding that at m/z 93 by a factor of 40. It is therefore clear that manipulating the drift voltage in this case could potentially distinguish between p-cymene and toluene, which would interfere at m/z 93. Steeghs et al. [8] reported the possibility of partial monoterpene differentiation by means of Collision Induced Dissociation (CID) in the Proton-Transfer-Reaction Ion Trap Mass Spectrometer (PIT-MS). The authors provided some information on monoterpene fragmentation, focusing on the m/z 95 fragment, but the method has not been finalised other than to point out the possibility of discrimination by PIT-MS.

This paper presents a new method, referred to as alternating drift (AD) mode, employing a standard PTR-MS without any modifications, which is shown to have the potential to discriminate monoterpenes (and other isomers) under alternating drift-tube voltage. In AD mode the drift voltage was made to change by a set time step per cycle in the range 400–600 V. For a drift-tube pressure (p_d) of 200 Pa and temperature (Td) of 318 K this range corresponds to 93–139 Td. Such a range offers a sufficient energy span to cause all parent monoterpene ions to fragment at the higher end of the Td range, but with a prevalence of molecular ions at the lower end of the Td range. In between, different monoterpenes fragment at different drift energies. The relative proportions of each monoterpene can in theory be deduced from the detailed fragmentation patterns as a function of the changing drift voltage. It should be noted that the dependence of monoterpene signals on humidity increases on lowering the drift energies because of second-order reactions and a very high number of clusters. This can be an advantage for distinguishing individual monoterpenes, as the water clusters with monoterpenes form adducts constituting more or less specific patterns in the fragment ions.

2. Design of an alternating drift PTR-MS (AD-PTR-MS)

The drift voltage (U_d) was cycled from 400 V to 600 V in 25 V time steps (dU_d). Once the value of U_d reached its maximum value of 600 V the voltage was reduced in 25 V time steps and the cycle repeated. This permitted the capture of the m/z spectrum from 21 to 206 amu with a relatively long acquisition time, for example 1.5 min per scan at 0.5 s dwell time, providing 18 data points per AD cycle and therefore two replicates for each voltage (i.e. 9 ascending voltages and 9 descending voltages). Such an approach gives approximately 25 min for the full AD mode, where the rest of the hour could be devoted, for example in the field, to eddy covariance flux measurement, and zero-air sampling. At least one zero air AD scan is required for subtraction of the background signal from the ambient AD spectra.

The high-sensitivity PTR-MS (Ionicon, s/n: 04-03) employed in the study has three Varian turbo pumps, Pfeiffer quadrupole mass filter (QMA 400) and a secondary electron multiplier (Pfeiffer SEM-217) coupled to an ion-count preamplifier (Pfeiffer CP-400) and Pfeiffer QMH400 RF box. A more detailed description of PTR-MS in general [9,10] and of this particular model [e.g. 11,12], can be found elsewhere. The Balzer sequencer of the quadrupole mass spectrometer of the PTR-MS was programmed to provide the cyclical change in U_d (see Supplement S-1). The changes in U_d resulted in characteristic profiles of the first water cluster signal (m/z 37), and also affected primary ions and other m/z intensities (Fig. 1).

The variation of U_d varies the E/N ratio, and hence varies the collision energies, which in turn affect fragmentation. In the AD-PTR-MS mode protonated water clusters vary greatly from below 1% of the primary ions at U_d = 600 V to as much as 20% at U_d = 400 V. These changes are beneficial for elucidation of isomer-specific fragmentation features since collisions with protonated water clusters provide additional opportunity for fragmentation and also for the creation of molecular clusters, which is likely to occur at

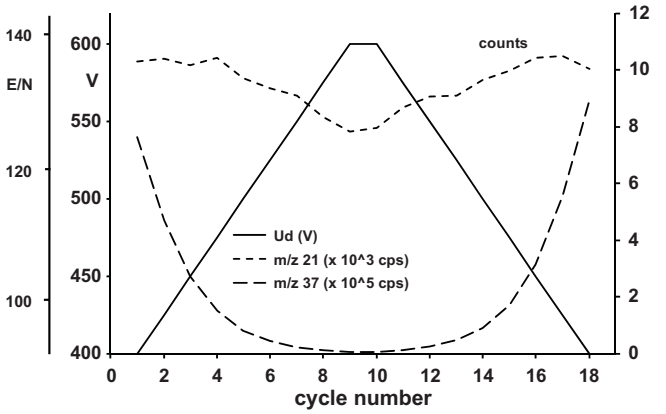

Fig. 1. Alternating U_{drift} design consisting of 9 ascending and 9 descending drift voltage steps (a full AD period), showing changes in primary ions (m/z 21) and water cluster (m/z 37) for conditions: water flow 6.5 sccm, drift tube pressure 200 Pa, temperature 45 °C. Values of E/N (Td) are also shown for comparison.

different drift voltages for different isomers. The simple analysis of the main fragments selected from the scan is already sufficient in many cases to discriminate between isomers measured in AD-PTR-MS. However, application of multivariate factor analysis such as positive matrix factorisation (PMF) is ideal for the recognition of the AD-PTR-MS scans and is described in detail below.

3. Methods

3.1. AD calibration

For the AD-PTR-MS calibration the drift pressure was maintained constant at 200 Pa, drift temperature at 45 °C, and the water vapour flow to the hollow cathode at 6.5 sccm. The U_d was alternated between 400 V and 600 V (equivalent E/N from 93 to 139 Td) as described in the previous section. Samples of individual monoterpenes were vaporised in clean Tedlar® bags filled with 3 L VOC-free air by injecting 2 μL of an ultrapure liquid standard (Sigma Aldrich, UK). The resulting volume mixing ratio (~700 ppb) was expected to be high enough to ensure the domination of the m/z spectrum by a given monoterpene but not high enough to cause a decline in primary ions. The air flow in the PTR-MS inlet was reduced from 300 mL min^{-1} to 50 mL min^{-1} which was sufficient to perform a full AD cycle (1 ascending and 1 descending voltage ramp) withdrawing less than half the gas from a bag. Altogether six monoterpenes (α-pinene, β-pinene, D-limonene, 3-carene, γ-terpinene, and α-phellandrene) and one monoterpene-related compound (p-cymene) were prepared (Fig. 2), each in separate identical bags (7 bags in total + 1 bag with zero air).

A zero-air generator (Sonimix 3052B) provided dilution gas for all the bags and removed all VOCs from the ambient (laboratory) air to below the limit of detection, except for methanol, whose count rate constituted 0.05% of the primary ions. Only a small portion of the count rate at m/z 33 corresponded to true ambient methanol, as the background at this ion channel is typically high compared with alternative Pt/Al_2O_3-based zero-air systems. The amount of methanol detected in the bags was insignificant relative to the concentrations of the monoterpenes used in the study, and was similar for all bags. The Sonimix 3052B generator has slightly better removal efficiency for compounds above 45 amu and generates substantially higher flow rates than alternative zero-air generators. All bags were analysed on a single day, starting with the bag containing only the zero-air.

After each experiment in AD-mode, with scans between m/z 21 and 206 at each selected U_d, the bag was detached from the

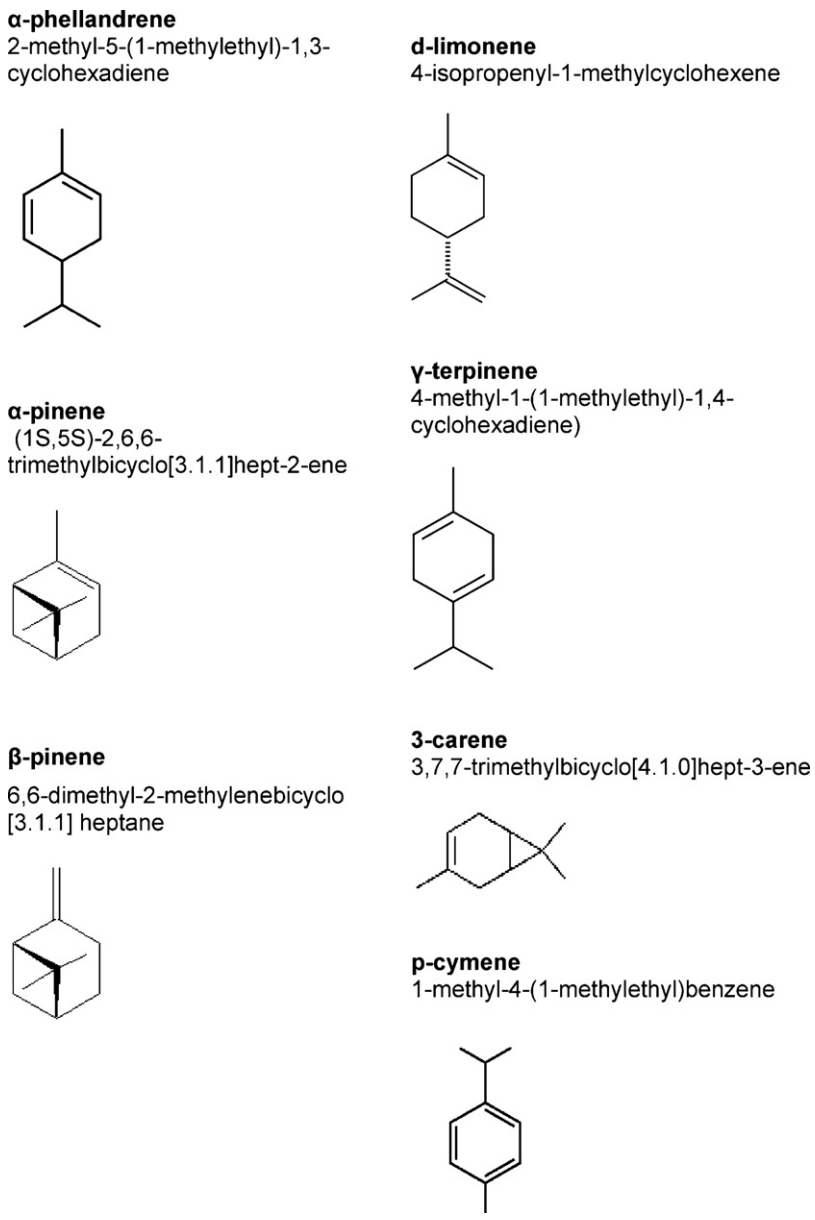

Fig. 2. Systematic names and structures of compounds used in the study.

instrument and the PTR-MS was flushed with zero-air, sampled directly, for at least 15 min before another bag was connected. The AD experiment with β-pinene was repeated on the following day from the same bag (stored in the dark), in order to check for the amount of variability between dates. The AD patterns for the main fragments were almost identical, although the whole spectrum contained somewhat more small peaks than earlier, and the normalised absolute values of the main fragments were very slightly smaller, which could be due to degradation of the standard during storage.

3.2. Postprocessing

A LabVIEW program was written for data analysis which automatically read the Balzer scan files, and normalised the count rates for each m/z cycle to 1×10^6 cps of the primary ions and protonated water cluster at m/z 37. In addition, each experiment had a corresponding cycle of the zero-air bag subtracted and returned three arrays: absolute count rates, count rates normalised only for primary ions, and count rates normalised for both the primary ions and protonated water clusters. Normalised count rates (ncps) were derived as in Eq. (1), whereas normalised count rates for both the primary and water-cluster ions (ncps_w) were derived as in Eq. (2).

$$I_{\mathrm{ncps}} = d_{\mathrm{norm}} \cdot \frac{I_{\mathrm{cps}} \cdot I_{\mathrm{ZAm}/z21} - I_{\mathrm{ZAcps}} \cdot I_{m/z21}}{I_{m/z21} \cdot I_{\mathrm{ZAm}/z21}} \quad (1)$$

$$I_{\mathrm{ncps\_w}} = d_{\mathrm{norm}} \cdot \frac{I_{\mathrm{cps}} \cdot \left(I_{\mathrm{ZAm}/z21} + I_{\mathrm{ZAm}/z37}\right) - I_{\mathrm{ZAcps}} \cdot \left(I_{m/z21} + I_{m/z37}\right)}{\left(I_{m/z21} + I_{m/z37}\right) \cdot \left(I_{\mathrm{ZAm}/z21} + I_{\mathrm{ZAm}/z37}\right)} \quad (2)$$

In these equations, I_{cps} and I_{ZAcps} are the signals in cps from a monoterpene and corresponding zero-air, respectively, while $I_{m/z21}$ and $I_{\mathrm{ZAm}/z21}$ are the corresponding signals at m/z_{21} from a monoterpene and the zero-air, respectively. The normalisation constant d_{norm} is equal to 2000 ncps, accounting for the 1×10^6 ncps normalisation level of primary ions divided by an approximate m/z 19:21 isotopic ratio of 500 corresponding to the abundance ratio between $H_3{}^{16}O^+$ and $H_3{}^{18}O^+$. The parameters $I_{m/z37}$ and $I_{\mathrm{ZAm}/z37}$

denote protonated water-cluster $[H_3{}^{16}O{\cdot}H_2{}^{16}O]^+$ count rates at m/z 37 ion channels from a monoterpene and the zero-air, respectively.

The analysis of the fragmentation patterns had two stages: analysis of the selected fragments, and the covariate analysis of the whole pattern.

The first stage consisted of the selection of the most abundant ions in the mass spectra (neglecting m/z ratios which had less than 0.05% abundance), then the derivation of their dependence on U_d, and finally the determination of 'critical' voltages at which major changes in fragmentation occurred. These were identified from sudden changes in slope in plots of abundance vs. U_d, or from points of intersection of tangents to the curve (see Fig. 4 for examples), and served as potential markers for subsequent discrimination of the different monoterpenes. The selected protonated ions were at m/z 137, 121, 93, 81, 79, 67, 57, 41, and 39. All these ions have been recognised as specific to monoterpenes, based on their high abundance, and it was subsequently confirmed in the PMF analysis (see Section 4.2) that these ions had the highest coefficient of determination (r^2) of the observed and predicted values in the PMF model. However, m/z 95 and m/z 88, despite their elevated abundance, were regarded as pollution from the material of Tedlar® bags [13], where the latter is most likely N,N-dimethylacetamide used in its production. Tani et al. [6], using a thermal diffusion approach of the pure standards, identified ions at m/z 71, 93, 97, 109 and 119 as impurities and used ions at m/z 67, 68, 81, 82, 95, 96, 137 and 138 in the analysis for monoterpenes. On the other hand, Maleknia et al. [7] used protonated masses 93, 95, 107, 109, 119, 121 and 137 in referring to terpenes.

In the AD approach presented here the selection of the protonated masses was justified as follows: the ion $C_9H_{13}{}^+$ at m/z 121 might be important as the fragment remaining after loss of CH_4 from a parent monoterpene ion $C_{10}H_{17}{}^+$ (m/z 137); for p-cymene $C_{10}H_{15}{}^+$ (m/z 135) a similar loss would lead to $C_9H_{11}{}^+$ at m/z 119, so 135 and 119 ion were added to the p-cymene analysis. Many of the fragments might coincide with either impurities or other common masses such as higher-order protonated water clusters. This can be recognised from AD graphs of U_d dependence and factor analysis, which can extract common features of many fragments together. However, for calibration purposes it is sensible to use sufficiently high concentrations that such interferences are of little quantitative importance. Assuming m/z 37 constitutes 1% of the primary ions, the contribution from protonated water clusters to m/z 39 would be around 0.005% of primary ions so approximately 50 cps normalised to 1×10^6 cps. If 1% of monoterpene fragments to m/z 39, and assuming 5 times higher sensitivity for monoterpenes at this m/z than at m/z 137, then approximately 5 ppb of monoterpene would be needed to exceed the contribution from the protonated water cluster signal. The signal related to protonated water clusters at m/z 37 could alternatively be converted using the isotopic ratio and subtracted from the m/z 39 signal in the AD spectra. Typically the m/z 41 ($C_3H_5{}^+$) fragment is elevated, which could represent propadiene or cyclopropene in monoterpene-rich atmospheres. Another interesting fragment which dominates monoterpene spectra occurs at m/z 67 ($C_5H_7{}^+$), which could be either cyclopentadiene or [1.1.1] propellane. It was rather surprising to observe m/z 79 (benzene) for some monoterpenes (e.g. >1% in α-phellandrene). Previously it has only been reported as contributing to 14% of fragments of adamantane ($C_{10}H_{16}$) [8] but has not yet been described as a monoterpene fragment, possibly because of an assumption that it might be present as an impurity in the standard. However, the relationship of the m/z 79 signal in response to the change in U_d suggests that it is benzene or, less likely, a fragment isomeric to benzene (e.g. bicyclopropenyl), formed when the C_4H_{10} (butane, isobutane) moiety is lost from a monoterpene. Given the theoretical stability of bicyclopropenyl [14], it is possible that it fragments further in order to form a very short lived cyclopropenylidene or other isomeric $C_3H_2{-}H^+$ ion at m/z 39. Further fragmentation of benzene is not favoured in the soft ionization offered by PTR-MS [15,16].

The data were normalised and expressed as the relative percentage of the sum of the ions selected, but the normalised count rates were not corrected for transmission response. Normally, transmission is derived by a measurement under constant E/N, so for this study no transmission correction has been made but, in general, derivation of a transmission response in the AD-mode might be useful. However, the relative differences of the voltage-dependent changes should be the same in all cases despite different absolute differences. Normally the transmission of ions starts to decline rapidly after 100 amu due to the fringing field effect [17], so a transmission-corrected signal would be higher at the larger m/z; for example at m/z 137 it should be around 2.5 times higher than without the correction (as used here). Different monoterpenes are likely to have a similar transmission response, but the uncertainty in the proton transfer reaction rates for each of them could introduce a bias. So the method presented here is principally qualitative. If the method can reproduce the relative proportions of isomers, then the absolute concentration could be derived by comparison with the classical calibration approach for the sum of monoterpene concentrations.

3.3. Double-blind trial

An analysis of unknown samples was performed under the same conditions as those during the AD calibration but the concentrations were much lower, in order to bring the challenge of discrimination closer to ambient levels. All 6 bags previously used in calibration, containing approx. 700 ppb of each monoterpenes (p-cymene bag excluded) were selected. Four of them were selected at random by a person not involved in the experiment, who labelled them A1, A2, A3 and A4. Four brand new bags flushed 5 times with zero-air were filled with approximately 3 L of zero-air. Subsequently, 50 mL of A3 monoterpene was injected to the first bag, 50 mL of A1 to the second, and the third bag was prepared to contain a mixture of A2 and A4 monoterpenes (25 mL each). The last new bag was left to serve as the first zero-air run. Therefore bags contained approximately 10 ppb of monoterpene, which was at the limit of detection for some small fragments.

3.4. Positive matrix factorisation

Positive Matrix Factorisation (PMF) has been employed successfully for the interpretation of the organic components of aerosol mass spectrometric data [18]. It has also been applied to PTR-MS fragmentation patterns [19]. The original PMF model [20,21] assumes that a measured dataset fulfils mass balance conservation of a number of constant source profiles of the concentration of species variable in time. The concentrations of species vary over time under constant reaction chamber parameters (sensitivity, fragmentation). Application of PMF to AD-PTR-MS mass spectra requires different assumptions, namely that the concentration of a species is assumed to be constant during an AD experiment, which is relatively short, but the E/N ratio is variable as affected by the alternating U_d. For this part of the experiment, additional hypotheses were assumed: (1) the factors and their profiles found by PMF in AD-PTR-MS can be related to the structure of an isomer, and (2) the common factors have different relationships with the drift voltage.

The PMF analysis utilised the program EPA PMF 3.0 [22], designed for receptor modelling of air quality data. The AD-PTR-MS data, normalised for m/z 19 and 37 and with zero-air data subtracted, were used as matrix **X** input (see Supplement S-2 for details). The occasional small negative values resulting from zero-air subtraction (within the noise of the data) were replaced by zeros. The EPA PMF 3.0 program also requires a file with uncertainties and

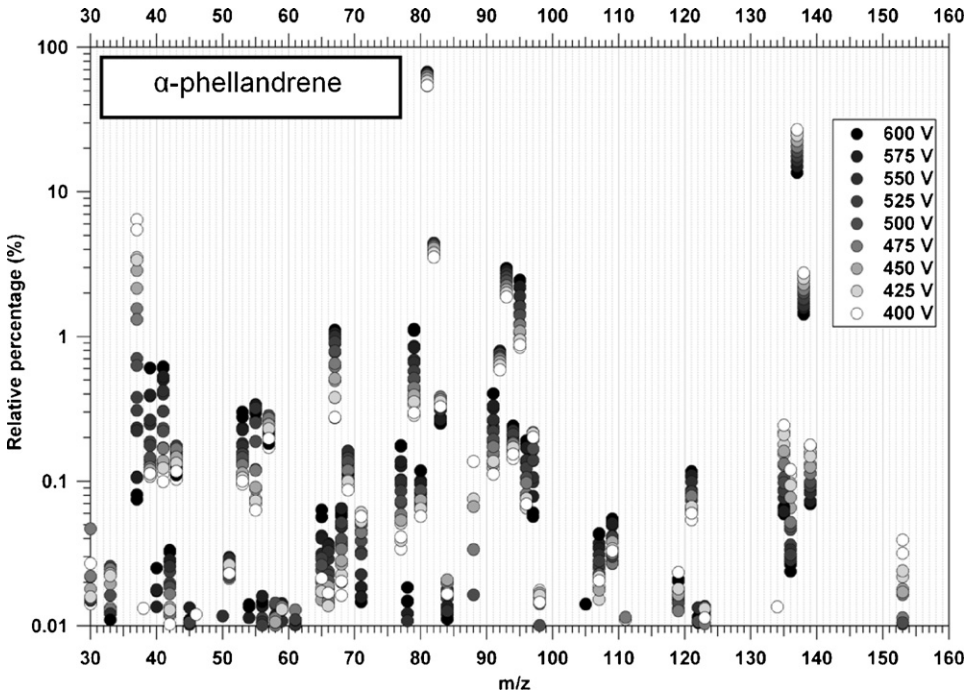

Fig. 3. Fragmentation patterns for α-phellandrene ($C_{10}H_{16}$) in relation to drift voltage (grey scale), with drift pressure maintained constant at 200 Pa, drift temperature at 45 °C, and the water vapour flow to the hollow cathode at 6.5 sccm. At this temperature and pressure the ratio of E/N to drift voltage (U_d) is given by $E/N = 0.231\ U_d$ (Fig. 1).

detection limits. For consistency and simplicity, a universal value of 10 ncps was set for all m/z as the detection limit, while the error of determination was set for all to 1%.

4. Results

4.1. AD patterns – differences in fragmentation

The variation in fragmentation throughout the AD cycle is shown for α-phellandrene in Fig. 3. Inspection of the AD patterns for all the investigated compounds (see Supplement, Fig. S1) shows that reliance only on the usual m/z values for monoterpenes (81 and 137) under a constant U_d is insufficient to identify a specific monoterpene. However, characteristic patterns can be seen in values of U_d at which significant changes in fragmentation occur (e.g. α-phellandrene, Fig. 4), which can be visualised on individual graphs for the most important fragments (see Supplement, Fig. S2), and in the factors derived from PMF analysis and their behaviour with U_d (see Section 4.2). For example, variability in the relative abundance of m/z 81 in α-pinene (or β-pinene) is significantly different from the corresponding variability in D-limonene; there is significantly elevated m/z 153 ion in γ-terpinene, also present but at lower level in α-phellandrene and D-limonene, and reaching highest abundances at the lower E/N ratio regions. These monoterpenes have an atmospheric lifetime of the order of tens of minutes, while the pinenes or carenes have lifetimes of the order of hours [23] so m/z 153 (137 + 16) could indicate an oxygenated molecule, which could have formed in the bag or following exposure to the drift-tube temperature. Impurities in the standard must also be considered a possibility. However, m/z 81 and 137 together constitute typically more than 95% of fragments; at low mixing ratios reliance on other fragments may be unreliable because of detection limits. The use of m/z 81 and 137 together for differentiation is described in Section 4.3. Detailed results follow for each of the studied compounds, measured in 'calibration' mode at ca. 700 ppb. Structures and systematic names are shown in Fig. 2.

4.1.1. α-Phellandrene

One of the main features of this monoterpene is that it has a hexadienyl ring but does not have any double bonds in its alkyl radicals. The principal fragmentation with characteristic critical voltages ($U_{dc\_m/z}$) is presented in Fig. 5. The critical voltages $U_{dc\_m/z}$ denoted as superscripts to the m/z values (Fig. 4) are as follows: (a) $U_{dc\_137} = 475$ V; (b) $U_{dc\_121} = 510$ V; (c) $U_{dc\_93a} = 440$ V; (d) $U_{dc\_81} = 475$ V; (e) $U_{dc\_79} = 555$ V; (f) $U_{dc\_67} = 525$; (g) $U_{dc\_57} = 500$ V; (h) $U_{dc\_41} = 490$ V; $U_{dc\_39} = 550$ V. These voltages were derived by analysing the dependence of the relative proportion of the fragment versus U_d either by calculating the intersection of the lines tangential to the curve or by extrapolating the U_d value if the curve has an evident peak or trough (e.g., as in m/z 57 in Fig. 4). The equivalent values for E/N under the experimental conditions can be obtained by multiplying U_d by 0.2312 (Td/V).

4.1.2. α-Pinene

The major fragments are the same as for α-phellandrene. The only differences are in the critical voltages or the shape of the dependence of the abundance of a given fragment on U_d. The α-pinene molecule has only one double bond in the cyclohexenyl ring, a tertiary carbon and a similar conformation of the methyl substituent to that of α-phellandrene. Therefore differences would be expected in m/z 57, which is probably a product of the two substituents (C1 + C3) detached from the ring. The formation of this adduct at m/z 57 increases until approximately 450 V (E/N 104 Td) and then it becomes stabilised (see Supplement S2a), before the ionization energy at about 550 V (E/N 127 Td) further fragments this molecule. At 550 V there is also a sudden increase in m/z 79 and m/z 39, which is probably an effect of dehydrogenation [$-H_2$] leading to formation of stable benzene from cyclohexadienyl fragment (m/z 81) and cyclopropenylidene from the carbenium ion (m/z 41). In the light of this, it is unlikely that m/z 79 is bicyclopropenyl since it is extremely unstable and would lead to a decrease in m/z 79 due to dissociation. It is possible that high E/N conditions (high voltages) enable certain fragmented moieties to undergo cyclisation and/or proton-bound dimerisation (typical for low E/N), but which will not

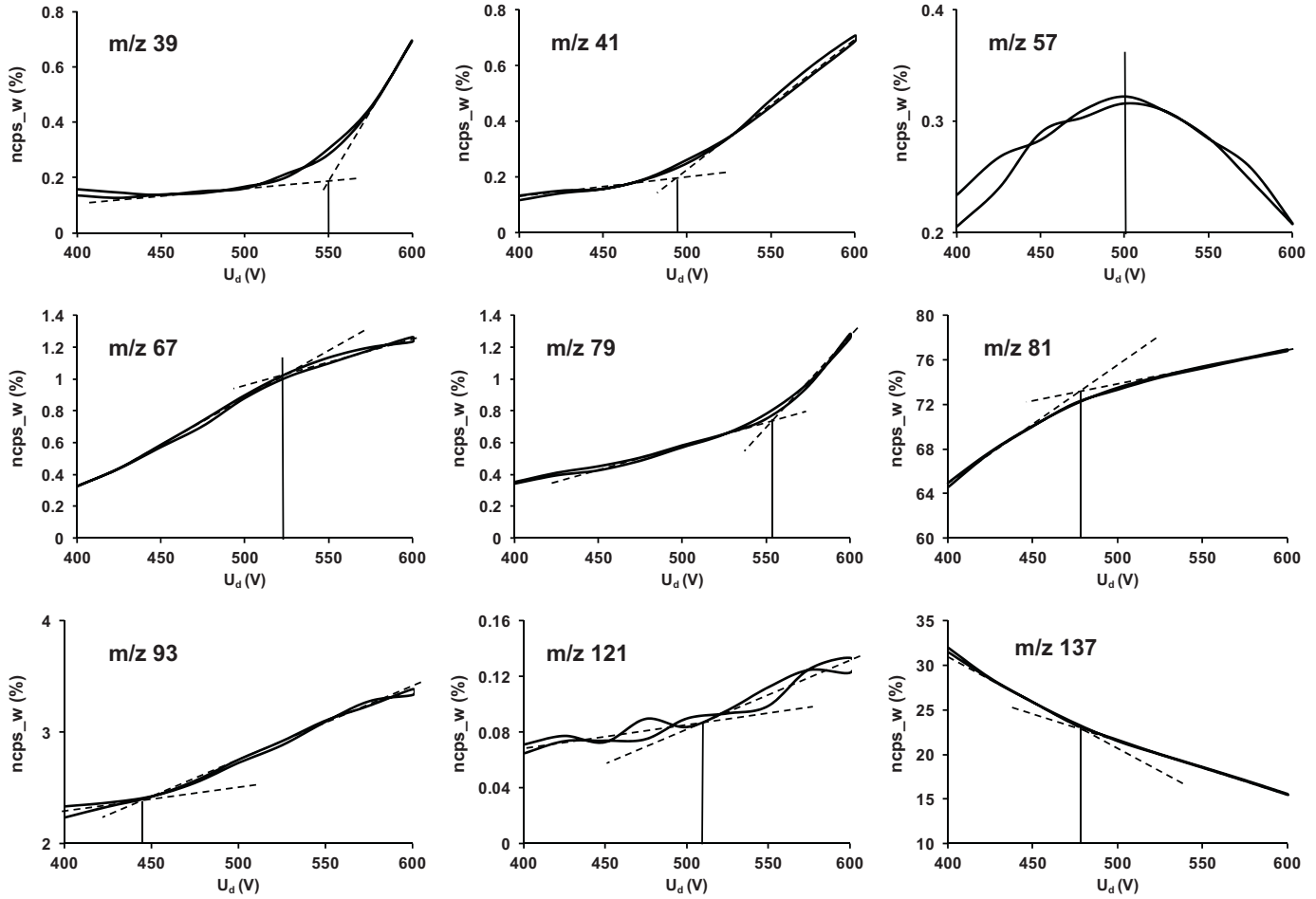

Fig. 4. Variability with U_d and distributions of the key ions (as relative abundance) in AD-PTR-MS of α-phellandrene. Characteristic voltages at which there are inflexions in the relationship between abundance and U_d are shown by drop lines. At 200 Pa and 45 °C the ratio of E/N to drift voltage (U_d) is given by $E/N = 0.231\ U_d$ (Fig. 1).

dissociate even at high energy because of the exceptional stability of the proton-bound adduct [24]. However, the most important feature is the linear relationship between the abundance of m/z 137 and U_d, a feature shared only with β-pinene.

4.1.3. β-Pinene

The m/z intensities as a function of U_d for β-pinene (see Supplement S2b) show many similar features to those of α-pinene, such as the near linearity for m/z 137 and the increase in m/z 79 and C_3H_2–H^+ at m/z 39 sharply increasing after 550 V. However, compared with α-pinene there is much lower abundance at m/z 57, and m/z 121 exhibits a much clearer signal. This is the only monoterpene without double bonds in the ring, which may explain the low relative abundance of toluene at m/z 93.

4.1.4. D-limonene

A unique feature of this monoterpene molecule is the presence of the isopropenyl group connected to the cyclohexenyl ring. The distribution of the parent ion m/z 137 (see Supplement S2c) is the most skewed to the left in comparison with all other monoterpenes, so it is highly probable that the isopropenyl substituent makes this structure the least resistant to fragmentation.

4.1.5. γ-Terpinene

The structure of γ-terpinene is similar to that of α-phellandrene, differing only in the position of one of the two double bonds in the ring. This relatively minor difference in the structure is important for γ-terpinene fragmentation in the AD mode, showing different responses for isopropyl fragment detachment (m/z 41) which in turn affects the rate of isopropylbenzene (m/z 121) and benzyl (m/z 93) formation. In the patterns of targeted ions for γ-terpinene (see Supplement S2d) one can observe an approximately 5 times higher relative proportion of m/z 121 than encountered for α-phellandrene, which suggests that the presence of the double bond next to isopropyl makes this substituent more resistant to detachment. The benzyl fragmentation shows upward curvature with a centre around 500 V and the opposite but more pronounced pattern in m/z 121. The detached isopropyl seems to cluster with abundant methyl ions, as seen in the pattern in m/z 57, which gives a unique pattern compared with α-phellandrene and other monoterpenes.

4.1.6. 3-Carene

The structure of 3-carene lacks double bonds in the substituents, similar to α-phellandrene, α-pinene, and γ-terpinene. The hexenyl ring is also only present in D-limonene and α-pinene, with the latter also having only one double bond. The AD patterns (see Supplement S2e) suggest that toluene (m/z 93) is easily formed, and in proportion to U_d. The pattern for m/z 121 resembles that of γ-terpinene. For m/z 67, which results from ring fragmentation, there is a plateau above about 550 V, as for the other monoterpenes except for D-limonene.

4.1.7. p-Cymene

p-cymene is not a monoterpene, but only differs in the presence of the aromatic ring, which is responsible for the shift in the

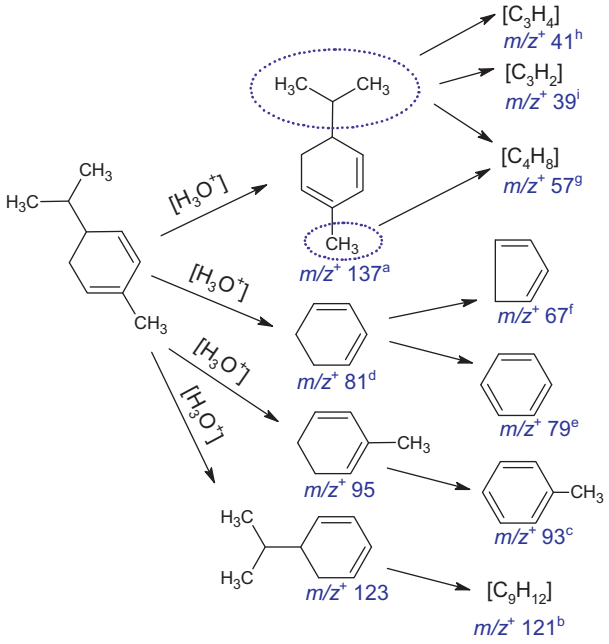

Fig. 5. Schematic for the fragmentation of monoterpenes in PTR-MS, using α-phellandrene as example. The m/z^+ values refer to the protonated fragments, not the neutral molecules as shown. The superscripts at each m/z^+ (except for 95 because of possible interference from Tedlar™ bag material, and 123 which was below 0.1%) refer to the characteristic $U_{dc,m/z}$ for α-phellandrene, which are further explained in the text. The structures of the protonated fragment ions are unknown.

fragmentation giving high abundances on different m/z ion channels, even in the absence of AD mode. There are several analogues in fragmentation in AD mode (see Supplement S2f), as many ions are encountered at $(m/z - 2)$ compared with monoterpenes. For example, the parent ion is now detected at m/z 135; the second most abundant fragment is toluene at m/z 93, and not benzene (m/z 79) as expected by analogy with m/z 81 in monoterpenes. This must be because of the exceptional stability of toluene formed after collisional dissociation, resulting in the loss of an isopropyl fragment. The detachment of the methyl substituent is also possible although the abundance at m/z 119 (analogous to m/z 121 in monoterpenes) is not high. The lack of parent ion m/z 135 above 550 V is very different to the analogue at m/z 137 in the monoterpenes. The m/z 93 ion ranges from about 50–85% of the abundance of the sum of the selected most abundant ions. The formation of toluene seems to reach saturation at about 550 V and then starts to decrease.

4.2. PMF results

One of the most important tasks with PMF is to identify the number of factors (p) in the dataset, which is unknown *a priori*. Four factors were identified for this dataset; example factor profiles and contributions of individual factors are shown in the Supplement Figs. S4 and S5, respectively. The relationships between the different factors and U_d (Fig. 6) suggest that they differ only in their relative proportions as a function of U_d. Factor 1 can be related to the overall degree of fragmentation, and is specific for a given monoterpene structure, which fragments with different abundance at different U_d. Factor 2 may denote clustering and/or dependence on humidity. Anticipating Section 4.3, this factor might not be specific to monoterpenes, probably because of interferences from water or other clusters, or second-order reactions which might explain the hysteresis of the factor 2 curve in the lower U_d range, i.e. different for ascending and descending part of the AD cycle. Factors 3 and 4 may refer to specific structural features of the isomers. It appears that these factors do not only occur in monoterpenes since similar representation can be observed for p-cymene.

Factor 1 can be presented as a fragmentation profile (see Supplement, Fig. S6) which clearly shows the power of its discrimination capabilities, showing large differences in m/z 81, 137, 95, 67, 79 and 39 and others. Factor 1 is completely different for p-cymene despite the similarities found with the monoterpenes (Fig. 6). Factor 2 shows large differences in m/z 37, which are probably not specific to the structure. Although the significance of factors 3 and 4 is unknown, their potential for discrimination may also be quite high. Generally, all factor profiles show differences in the channels of highest abundance, i.e. m/z 137 and m/z 81.

4.3. Identification experiment (double blind trial)

Discriminating features can be found in the relatively small fragments of the spectra, which may not be practically useful at the low concentrations typical of ambient air, or even at 10 ppb as used in the identification experiment. In the identification experiments the AD patterns were noisier than for the calibration experiments at 700 ppb, with fewer non-zero values of m/z. Nevertheless, many of the characteristic features and differences were retained.

4.3.1. Use of ratios of abundances and PMF factors

In order for the AD approach to discriminate monoterpenes at low concentrations, only the most abundant m/z (i.e. 81 and 137) or their ratio can be used. The relative proportion between m/z 81 and m/z 137 changes with the E/N ratio, but the absolute values of those proportions for a range of E/N ratios for each monoterpene isomer have not been tested. The normalised data for the full AD cycle were summed, and the ratios of m/z 81 to m/z 137 ($K_{AD81/137}$) are presented in Table 1 for the 6 monoterpenes tested, in comparison with the data for the unknown monoterpenes. In addition, the ratios of m/z 81 to m/z 137 in the spectra of the four PMF factors ($F_{1\text{-}AD81/137}$ … $F_{4\text{-}AD81/137}$) are also presented; these had different values for a given monoterpene in the calibration. The data for both the calibration and unknown compounds are listed in Table 1. However, not all the factors behave similarly at both high and low concentrations, and so are of limited use for practical discrimination. All the $F_{2\text{-}AD81/137}$ values for unknown monoterpenes were much smaller than those derived in calibration, suggesting a particular dependence on the absolute concentrations of m/z 37.

The analysis of characteristic voltages (e.g. Fig. 4), could be used only on high concentration data, so a scoring system was applied to identify the compounds from the double-blind trial based solely on the $K_{AD81/137}$ and $F_{n\text{-}81/137}$ values. The closest match of an unknown to a known component was awarded 2 points; any further match(es) were awarded 1 point, provided that no value was outside a ±0.3 window. If all values were outside the window then no score was awarded. A1 received 6 points towards being α-phellandrene, 2 points towards α-pinene, and only 1 point towards β-pinene, identifying A1 as probably α-phellandrene. A3 obtained 4 points towards β-pinene, and also 4 points towards α-pinene, then 2 points towards 3-carene, 2 points for α-phellandrene, and 1 point for γ-terpinene, suggesting either α-pinene or β-pinene. Finally the mixture of two monoterpenes (A2 + A4) was rated 4 points that it contained γ-terpinene, 3 points that it contained 3-carene and 1 point for D-limonene.

4.3.2. Use of individual ion responses to changes in U_d

Using individual m/z data (see Supplement, Fig. S1), some patterns emerge that are also helpful for discrimination, particularly for m/z 81 and 137. The relationship between the abundance of m/z 137 and U_d is linear for A1 and A3 and curved for A2 + A4, implying that A1 and A3 could be pinenes or α-phellandrene, rather than D-limonene or γ-terpinene, which showed a curved response. The

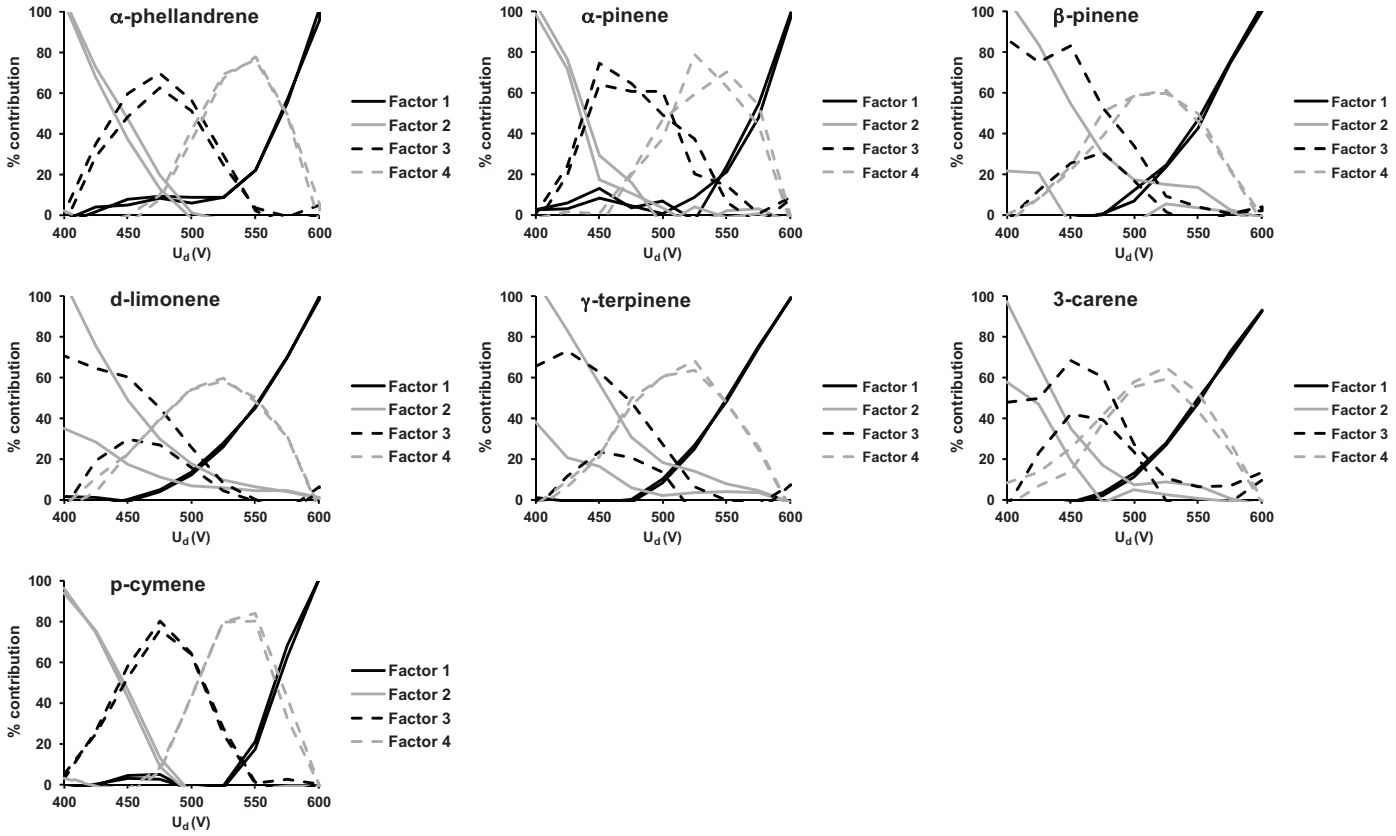

Fig. 6. Comparison between factor contributions for each monoterpene and p-cymene in relation to U_d. At 200 Pa and 45 °C the ratio of E/N to drift voltage (U_d) is given by $E/N = 0.231\ U_d$ (Fig. 1).

curvature of m/z 137 observed in the A2 + A4 mixture excludes the possibility of it containing only pinenes or α-phellandrene.

4.3.3. Use of abundance ratios response to changes in U_d

The variation of the ratio of m/z 81 to m/z 137 is approximately linear with U_d for each of the monoterpenes tested (Fig. 7). The pure compounds fall into two groups; γ-terpinene and 3-carene have generally lower ratios at all values of U_d compared to the other compounds, with γ-terpinene having a stronger response than 3-carene. In the other group, D-limonene has the strongest response, while α- and β-pinene are similar, and α-phellandrene is intermediate. Identification of an unknown through membership of one or other of the groups, and then by response to changes in U_d, should then be straightforward, although with ambiguities over

Table 1
Values of the mean ratios of m/z 81 and m/z 137 ($K_{AD81/137}$) for the integrated U_d range of 400–600 V for each monoterpene isomer used in AD calibration, and values derived for unknown monoterpenes in the DB trial. The superscript abbreviated labels point to possible isomers identified using a scoring system as described in the text. $K_{AD81/137}$ refers to the ratio of normalised counts; $F_{n\text{-}AD81/137}$ represents ratios from each of the four factor spectra.

Isomer name	γ-Terpinene	D-limonene	3-Carene	α-Pinene	β-Pinene	α-phellandrene
Abbreviation	ter	lim	car	apin	bpin	phel
Calibration						
Full						
$K_{AD81/137}$	2.42	3.80	2.13	2.84	3.05	3.20
Factorised						
$F_{1\text{-}AD81/137}$	3.89	6.71	3.43	3.99	4.26	4.96
$F_{2\text{-}AD81/137}$	1.41	2.13	1.24	2.20	2.43	2.08
$F_{3\text{-}AD81/137}$	1.46	2.31	1.73	2.68	2.48	3.09
$F_{4\text{-}AD81/137}$	2.92	4.87	2.47	3.35	3.38	3.96

Unknown isomer(s) label	A1	A3	A2 + A4
Identification			
Full			
$K_{AD81/137}$	3.48^{phel}	$3.04^{bpin,(apin,phel)}$	$2.34^{ter,(lim)}$
Factorised			
$F_{1\text{-}AD81/137}$	4.95^{phel}	$4.14^{bpin,(apin)}$	3.34^{car}
$F_{2\text{-}AD81/137}$	0.12	0.95	0.94
$F_{3\text{-}AD81/137}$	$2.74^{apin,(bpin)}$	$2.82^{apin,(phel)}$	$1.55^{ter,(car)}$
$F_{4\text{-}AD81/137}$	3.84^{phel}	$2.68^{car,(ter)}$	1.92

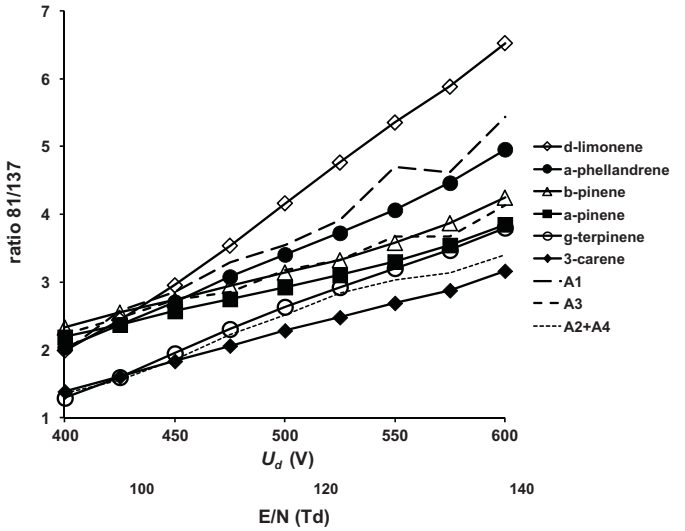

Fig. 7. Variation of the ratio of abundances of fragments at m/z 81 and m/z 137 as a function of voltage (U_d) for pure compounds at ca. 700 ppb, and for the 3 unknowns (A1, A3, A2 + A4) at concentrations of ca. 10 ppb. The equivalent values of E/N (Td) at 200 Pa and 45 °C are also shown.

the pinenes. Mixtures become more difficult to resolve, as there will in general be no unique solution. For example, the response of α-phellandrene would be similar to that of a mixture of D-limonene and a pinene, assuming no interactions between fragments of different monoterpenes. However, this response provides another line of evidence in deducing which monoterpenes may or may not be present in a mixture. In the case of the unknowns in this experiment, the single component A1 was identified as α-phellandrene, A3 as one of the pinenes, and the binary mixture (A2 + A4) as 3-carene and γ-terpinene. In the case of the mixture the random choice of this particular mixture fortuitously resulted in an unambiguous result, given that these are the only two of the compounds studied to have a low ratio across all the range of U_d.

4.3.4. Identity of unknowns

The identity of the unknown monoterpenes was revealed as: A1 - α-phellandrene, A2 - 3-carene, A3 - α-pinene, A4 - γ-terpinene. This means that the identification was successful, except for not being able to distinguish between the pinenes, and with the caveat that the binary mixture turned out to be a special case. The method needs to be tested in field experiments in conjunction with GC–MS to validate the uniqueness of the identification and of the scoring system proposed here.

5. Discussion

The results from the calibration experiment shed light on the behaviour of monoterpenes in the AD mode, which supplements current knowledge on their measurement by PTR-MS, and on fragmentation patterns to be expected with changes in U_d. These data are important in their own right, regardless of their utility in discriminating individual monoterpenes.

Schoon et al. [25] studied the reactions of H_3O^+ ions with selected monoterpenes using a selected ion flow tube (SIFT) at a low E/N ratio (80 Td). The monoterpenes in common with our study were α-pinene, β-pinene, limonene and 3-carene. Only 3 fragments were studied (m/z 81, 93 and 137) so all the fragment ratios could not be directly compared. However, the relative relationships of the fragment ratios scaled to our ratio for β-pinene (at E/N of 93 Td; U_d of 400 V) showed remarkable similarity for α-pinene and 3-carene, but was less similar for D-limonene for which the ratio declines rapidly towards lower E/N, as used by these authors (80 Td). Another SIFT-MS study was conducted by Wang et al. [26] for all the monoterpenes studied by us except for α-phellandrene. Although the exact E/N ratio was not stated in their report it is likely that it was also much lower than our lowest ratio (93 Td). The absolute values for the m/z 81/137 ratio were less similar than those of Schoon et al. [25] but the overall rank of the m/z 81/137 ratios was consistent, i.e. β-pinene > α-pinene > D-limonene > 3-carene > γ-terpinene. SIFT studies are valuable for studying proton transfer reactions, but the fragment ratios may not be directly comparable with those from the PTR-MS. Although perfect agreement would not be expected given the potentially different transmission characteristics and conditions (e.g. humidities) the m/z 81/137 ratios at 520 V (E/N 121 Td) in our study compared very well with those of Maleknia et al. [7] in their fragmentation study of monoterpenes at U_d of 580 V and E/N around 120 Td, for β-pinene (1% difference), α-pinene (27%), D-limonene (20%), and γ-terpinene (8%). It is surprising that these authors found such different m/z 81/137 ratios for the two pinenes (α - 2.3, β - 3.3) given their similar structures. However, the m/z 93 fragment in their study was extremely high (23%) for α-pinene whereas it is usually around 1%, as was the case for other monoterpenes.

The potential for identification of monoterpene isomers by AD-PTR-MS is illustrated by the following:

both the summed normalised spectra and the PMF profile spectra provide differences between each isomer tested, which may be more or less specific but which deliver additional qualitative information that is otherwise lacking in the commonly-used constant E/N PTR-MS mode;

characteristic voltages for each m/z fragment are the clue to differences in the spectra, although many specific features can be lost in the noise if the monoterpene concentration is small;

the use of abundance ratios in AD-PTR-MS has a promising potential for discrimination, even based on just normalised count rates of the summed AD cycle values, in the case of monoterpenes for the ratio of m/z 81 and m/z 137. This finding could warrant shortening the AD cycle to scan through the few m/z of interest, using longer dwell times to improve sensitivity. However, PMF requires the full spectra for elucidating the factors, of which relative ratios of contributions from m/z 81 and m/z 137 can further aid identification.

Although this method opens up possibilities that expand the utility of PTR-MS measurements without the need for further data from GC–MS analysis, several shortcomings are apparent, e.g. the difficulty in the discrimination of α-pinene and β-pinene. This might be possible using the additional information from the characteristic voltages if the signals were sufficiently clear. The purity of the standards used for calibration might be an issue if discrimination relied on the presence of low-abundance fragments. In any real atmospheric sample, contributions to the key fragment ions at m/z at 81 and/or 137 from compounds other than monoterpenes would also degrade the discriminating power of the approach. However, this initial study suggests a means of extracting qualitative, as well as quantitative, information from PTR-MS data.

6. Conclusions

Differences in monoterpene structures make it possible to distinguish isomers in the alternating E/N ratio mode using mass spectra, relationships between abundances of different m/z and the alternating drift voltage, and PMF analysis. However, the limit of detection can be an issue if minor fragments are lost in the interferences with other fragments or noise. One approach is to use the ratios of m/z 81 and 137 as a primary step of discrimination. The experiment suggests that reliance on the ratio of the abundances of

the two major ions ($K_{AD81/137}$) and of their weightings in the PMF factors ($F_{AD81/137}$) should be effective even on relatively small concentrations. The study has presented the first successful attempt to distinguish monoterpenes using a standard PTR-MS. Further studies with additional individual compounds are required to verify the uniqueness of $K_{AD81/137}$ and $F_{AD81/137}$ for all monoterpenes. In principle, the approach could also be used to discriminate among other compounds which are confounded in PTR-MS analysis, such as methyl vinyl ketone/methacrolein. Although the method extends the selectivity of a PTR-MS method it cannot compete with the gold standard of GC–MS identification.

Acknowledgements

Pawel Misztal was funded jointly by CEH and the School of Chemistry at the University of Edinburgh. The authors thank Sue Owen (CEH) for providing monoterpene standards for this work.

Appendix A. Supplementary data

Supplementary data associated with this article can be found, in the online version, at doi:10.1016/j.ijms.2011.11.001.

References

[1] W. Grabmer, M. Graus, C. Lindinger, A. Wisthaler, B. Rappengluck, R. Steinbrecher, A. Hansel, Disjunct eddy covariance measurements of monoterpene fluxes from a Norway spruce forest using PTR-MS, International Journal of Mass Spectrometry 239 (2004) 111–115.
[2] S. Hayward, A. Tani, S.M. Owen, C.N. Hewitt, Online analysis of volatile organic compound emissions from Sitka spruce (Picea sitchensis), Tree Physiology 24 (2004) 721–728.
[3] S.M. Noe, J. Penuelas, U. Niinemets, Monoterpene emissions from ornamental trees in urban areas: a case study of Barcelona, Spain, Plant Biology 10 (2008) 163–169.
[4] J. Penuelas, J. Llusia, I. Filella, Methyl salicylate fumigation increases monoterpene emission rates, Biologia Plantarum 51 (2007) 372–376.
[5] A. Tani, S. Hayward, A. Hansel, C.N. Hewitt, Effect of water vapour pressure on monoterpene measurements using proton transfer reaction-mass spectrometry (PTR-MS), International Journal of Mass Spectrometry 239 (2004) 161–169.
[6] A. Tani, S. Hayward, C.N. Hewitt, Measurement of monoterpenes and related compounds by proton transfer reaction-mass spectrometry (PTR-MS), International Journal of Mass Spectrometry 223 (2003) 561–578.
[7] S.D. Maleknia, T.L. Bell, M.A. Adams, PTR-MS analysis of reference and plant-emitted volatile organic compounds, International Journal of Mass Spectrometry 262 (2007) 203–210.
[8] M.M.L. Steeghs, E. Crespo, F.J.M. Harren, Collision induced dissociation study of 10 monoterpenes for identification in trace gas measurements using the newly developed proton-transfer reaction ion trap mass spectrometer, International Journal of Mass Spectrometry 263 (2007) 204–212.
[9] R.S. Blake, P.S. Monks, A.M. Ellis, Proton-transfer reaction mass spectrometry, Chemical Reviews 109 (2009) 861–896.
[10] W. Lindinger, A. Hansel, A. Jordan, On-line monitoring of volatile organic compounds at pptv levels by means of proton-transfer-reaction mass spectrometry (PTR-MS) – Medical applications, food control and environmental research, International Journal of Mass Spectrometry 173 (1998) 191–241.
[11] P.K. Misztal, S.M. Owen, A.B. Guenther, R. Rasmussen, C. Geron, P. Harley, G.J. Phillips, A. Ryan, D.P. Edwards, C.N. Hewitt, E. Nemitz, J. Siong, M.R. Heal, J.N. Cape, Large estragole fluxes from oil palms in Borneo, Atmospheric Chemistry and Physics 10 (2010) 4343–4358.
[12] B. Langford, P.K. Misztal, E. Nemitz, B. Davison, C. Helfter, T.A.M. Pugh, A.R. MacKenzie, S.F. Lim, C.N. Hewitt, Fluxes and concentrations of volatile organic compounds from a South-East Asian tropical rainforest, Atmospheric Chemistry and Physics 10 (2010) 8391–8412.
[13] M.M.L. Steeghs, S.M. Cristescu, F.J.M. Harren, The suitability of Tedlar bags for breath sampling in medical diagnostic research, Physiological Measurement 28 (2007) 73–84.
[14] T.C. Dinadayalane, U.D. Priyakumar, G.N. Sastry, Exploration of C_6H_6 potential energy surface: a computational effort to unravel the relative stabilities and synthetic feasibility of new benzene isomers, The Journal of Physical Chemistry A 108 (2004) 11433–11448.
[15] C. Ammann, C. Spirig, A. Neftel, M. Steinbacher, M. Komenda, A. Schaub, Application of PTR-MS for measurements of biogenic VOC in a deciduous forest, International Journal of Mass Spectrometry 239 (2004) 87–101.
[16] C. Warneke, C. van der Veen, S. Luxembourg, J.A. de Gouw, A. Kok, Measurements of benzene and toluene in ambient air using proton-transfer-reaction mass spectrometry: calibration humidity dependence, and field intercomparison, International Journal of Mass Spectrometry 207 (2001) 167–182.
[17] S. Kim, T. Karl, D. Helmig, R. Daly, R. Rasmussen, A. Guenther, Measurement of atmospheric sesquiterpenes by proton transfer reaction-mass spectrometry (PTR-MS), Atmospheric Measurement Techniques 2 (2009) 99–112.
[18] I.M. Ulbrich, M.R. Canagaratna, Q. Zhang, D.R. Worsnop, J.L. Jimenez, Interpretation of organic components from Positive Matrix Factorization of aerosol mass spectrometric data, Atmospheric Chemistry and Physics 9 (2009) 2891–2918.
[19] J.G. Slowik, A. Vlasenko, M. McGuire, G.J. Evans, J.P.D. Abbatt, Simultaneous factor analysis of organic particle and gas mass spectra: AMS and PTR-MS measurements at an urban site, Atmospheric Chemistry and Physics 10 (2010) 1969–1988.
[20] P. Paatero, Least squares formulation of robust non-negative factor analysis, Chemometrics and Intelligent Laboratory Systems 37 (1997) 23–35.
[21] P. Paatero, U. Tapper, Positive Matrix Factorization - a nonnegative factor model with optimal utilization of error-estimates of data values, Environmetrics 5 (1994) 111–126, EPA PMF 3.0 Software, v. 3.0.2.2, in, 2010.
[22] EPA, EPA PMF 3.0 Software, v. 3.0.2.2, in, 2010.
[23] R. Atkinson, J. Arey, Gas-phase tropospheric chemistry of biogenic volatile organic compounds: a review, Atmospheric Environment 37 (2003) S197–S219.
[24] H.E. Audier, J. Fossey, P. Mourgues, T.B. McMahon, S. Hammerum, Formation of proton-bound dimers as the driving force for alkyl radical loss in the gas phase reactions of radical cations, The Journal of Physical Chemistry 100 (1996) 18380–18386.
[25] N. Schoon, C. Amelynck, L. Vereecken, E. Arijs, A selected ion flow tube study of the reactions of H_3O^+, NO^+ and O_2^+ with a series of monoterpenes, International Journal of Mass Spectrometry 229 (2003) 231–240.
[26] T. Wang, P. Španěl, D. Smith, Selected ion flow tube, SIFT, studies of the reactions of H_3O^+ NO^+ and O_2^+ with eleven $C_{10}H_{16}$ monoterpenes, International Journal of Mass Spectrometry 228 (2003) 117–126.